



1 **Formation and Evolution of Secondary Organic Aerosol Derived from Urban Lifestyle Sources:**
2 **Vehicle Exhaust and Cooking Emission**

3 Zirui Zhang^{§,1}, Wenfei Zhu^{§,1}, Min Hu^{*,1,2,5}, Kefan Liu¹, Hui Wang¹, Rongzhi Tang¹, Ruizhe Shen¹, Ying Yu¹, Rui Tan¹, Kai
4 Song¹, Yuanju Li¹, Wenbin Zhang³, Zhou Zhang³, Hongming Xu³, Shijin Shuai³, Shuangde Li⁴, Yunfa Chen⁴, Jiayun Li⁶, Yuesi
5 Wang⁶, Song Guo¹

6 ¹State Key Joint Laboratory of Environmental Simulation and Pollution Control, International Joint Laboratory for Regional
7 Pollution Control, Ministry of Education (IJRC), College of Environmental Sciences and Engineering, Peking University,
8 Beijing 100871, China

9 ²Collaborative Innovation Center of Atmospheric Environment and Equipment Technology, Nanjing University of
10 Information Science & Technology, Nanjing 210044, China P. R.

11 ³State Key Laboratory of Automotive Safety and Energy, Tsinghua University, Beijing 100084, China

12 ⁴State Key Laboratory of Multiphase Complex Systems, Institute of Process Engineering, Chinese Academy of Sciences,
13 Beijing 100190, China

14 ⁵Beijing Innovation Center for Engineering Sciences and Advanced Technology, Peking University, Beijing 100871, China

15 ⁶State Key Laboratory of Atmospheric Boundary Layer Physics and Atmospheric Chemistry (LAPC), Institute of Atmospheric
16 Physics, Chinese Academy of Sciences, Beijing 100029, China

17 [§]These authors contributed equally to this work.

18 *Correspondence to: Min Hu (minhu@pku.edu.cn).*

19
20 **ABSTRACT**

21 Both vehicle exhaust and cooking emission are closely related to the daily life of city dwellers, which are considered as
22 major sources of urban secondary organic aerosol (SOA). Here, we defined the SOA derived from vehicle exhaust and cooking
23 emission as "Urban Lifestyle SOA", and simulated their formation using a Gothenburg potential aerosol mass reactor (Go:
24 PAM). After samples had been aged under 0.3-5.5 days of equivalent photochemical age, these two urban lifestyle SOA
25 showed markedly distinct features in SOA mass growth potentials, oxidation pathways and mass spectra. The SOA/POA mass
26 ratios of vehicle groups (107) were 44 times larger than those of cooking groups (2.38) at about 2 days of equivalent
27 photochemical age. It reveals that organics from vehicle may undergo the alcohol/peroxide and carboxylic acid oxidation
28 pathway to produce abundant less/more oxidized oxygenated OA (LO-OOA and MO-OOA), and only a few primary
29 hydrocarbon-like organic aerosol (HOA) remains unaged. In contrast, organics from cooking may undergo the
30 alcohol/peroxide oxidation pathway to produce moderate LO-OOA, and comparable primary cooking organic aerosol (COA)
31 remains unaged. Our findings provide an insight into atmospheric contributions and chemical evolutions for urban lifestyle
32 SOA, which would greatly influence the air quality and health risk assessments in urban areas.



33 1. Introduction

34 Organic aerosol (OA) contributes 20-90% of submicron aerosols in mass (Jimenez et al., 2009;Zhang et al., 2011), and
35 its fraction in urban areas is higher than that in suburban or background (Zhou et al., 2020). The OA could be divided into
36 primary organic aerosol (POA) and secondary organic aerosol (SOA). POA is directly emitted into ambient air through coal
37 combustion, biomass burning, vehicle exhaust, cooking procedure and so forth (Jimenez et al., 2009;Zhang et al., 2011;Zhou
38 et al., 2020). SOA is formed via the oxidation of gas-phase organics and the distribution between gas and particle phase
39 (Donahue et al., 2009). Significant SOA formation has been observed in several urban areas, but model failed to simulate this
40 phenomenon accurately (Matsui et al., 2009;Kleinman et al., 2008;Volkamer et al., 2006;de Gouw et al., 2008). This
41 discrepancy may attribute to the limited knowledge about the sources and characteristics of urban SOA.

42 Over the past decades, megacities have already been widespread in developed regions, and rapid urbanizations have been
43 sweeping across the globe especially in developing areas (Zhang et al., 2015). An increasing number of people tend to live in
44 the urban for their livelihood, where they suffer from serious air pollution simultaneously from urban lifestyle sources
45 typically involving vehicle and cooking fumes (An et al., 2019;Zhang et al., 2015;Chan and Yao, 2008;Guo et al., 2014;Guo
46 et al., 2020). For instance, polycyclic aromatic hydrocarbons (PAHs) are important carcinogens coming from vehicle and
47 cooking, which can cause severe lung cancer (Seow et al., 2000;Kim et al., 2015;Zhong et al., 1999). After PAHs are emitted
48 to ambient air, they would be oxidized, distributed into particle phase and finally become the part of POA or SOA, thus adding
49 unknown deviations on health risk assessments (Masuda et al., 2020).

50 Vehicle and cooking emissions are important sources of OA in urban areas (Rogge et al., 1991;Rogge et al., 1993;Hu et
51 al., 2015;Hallquist et al., 2016;Crippa et al., 2013;Mohr et al., 2012;Guo et al., 2013;Guo et al., 2012), take several megacities
52 for example, in London and Manchester, these two lifestyle sources contributed 50% and 54% of OA in average (Allan et al.,
53 2010). In addition, the vehicle itself could even contribute 62% of OA mass in rush hour of New York City (Sun et al., 2012).
54 As for OA source appointments in Paris, vehicle and cooking contributed maximum 46-50% of OA (Crippa et al., 2013).
55 According to seasonal observations in Beijing, there were at least 30% of OA coming from vehicle and cooking emissions
56 (Hu et al., 2017). Briefly, these two urban lifestyle sources are closely related to the daily life of city residents and could
57 account for 20-60% of ambient OA mass in urban areas when only considering their contributions to POA (Allan et al.,
58 2010;Sun et al., 2011;Ge et al., 2012;Sun et al., 2012;Lee et al., 2015;Hu et al., 2017). Furthermore, the model speculated that
59 vehicle and cooking emissions might even contribute over 90% of SOA in downtown Los Angeles by applying hypothetical
60 parameters with a certain degree of uncertainty (Hayes et al., 2015). Therefore, vehicle and cooking are momentous sources
61 of both POA and SOA in urban areas, and could be defined as “Urban Lifestyle Source of OA”.

62 As is well-known, large amounts of volatile, semi-volatile and intermediate-volatility organic compounds (VOCs,
63 SVOCs and IVOCs, respectively) are emitted from vehicle and cooking sources, leading to largely potential SOA productions
64 (Klein et al., 2016;Katragadda et al., 2010;Liu et al., 2017c;Tang et al., 2019;Zhao et al., 2015;Esmailirad and Hosseini,
65 2018;Zhao et al., 2017;Yu et al., 2020). Lab studies have investigated the formation of vehicle or cooking SOA using a smog



66 chamber or an oxidation flow reactor (OFR). On the one hand, some lab experiments have investigated the vehicle SOA based
67 on variables such as fuel types, engine types, operating conditions and so on (Deng et al., 2020; Suarez-Bertoa et al., 2015; Zhao
68 et al., 2015; Du et al., 2018). Several smog chamber results found that the mass loading of SOA exceeded POA when the
69 equivalent photochemical age was more than one day (Gordon et al., 2013; Chirico et al., 2010; Nordin et al., 2013). Besides,
70 OFR could simulate a higher OH exposure, and the peak SOA production occurred after 2-3 days of equivalent atmospheric
71 oxidation (Tkacik et al., 2014; Zhao et al., 2018; Timonen et al., 2017; Watne et al., 2018; Alanen et al., 2017). The mass spectra
72 of vehicle SOA showed both semi-volatile and low-volatility oxygenated organic aerosol (SV-OOA and LV-OOA) features
73 along with the growth of oxidation degree (Tkacik et al., 2014). On the other hand, only a few lab experiments have
74 investigated the cooking SOA based on simplified ingredients or a single cooking method, involving heated cooking oils (Liu
75 et al., 2017a; Liu et al., 2018), stir-frying spices (Liu et al., 2017b), charbroiled meat (Kaltsonoudis et al., 2017) and Chinese
76 cuisines (Zhang et al., 2020b). These lab experiments indicated that the characteristics of SOA are influenced by multiple
77 factors, such as cooking methods, fuels, cookers or ingredients. The mass ratios of POA and SOA derived from cooking are
78 comparable, and the mass spectra of SOA showed much more similarities with the ambient semi-volatile oxygenated OA (SV-
79 OOA) factors (Liu et al., 2018). Although these lab studies have provided important insights into the secondary formation of
80 vehicle and cooking SOA, significant uncertainties still exist. Nobody has compared the different natures generated from
81 these two urban lifestyle sources in detail, let alone pointed out their potentially different roles in the real atmosphere.

82 In this work, we have designed our vehicle and cooking lab experiments according to daily basis situations in urban areas
83 of China. For vehicle exhaust simulation, China V gasoline and three common operation conditions were chosen. For cooking
84 emission simulation, four prevalent Chinese domestic cooking types were evaluated. A Gothenburg potential aerosol mass
85 reactor (Go: PAM) was used as the oxidation system. All the fresh or aged OA was characterized in terms of mass growth
86 potentials, elemental ratios, oxidation pathways and mass spectra. The aged OA could be divided into POA and SOA. The
87 latter was defined as “Urban Lifestyle SOA” whose mass spectra would be compared with those of ambient SOA, like less-
88 oxidized oxygenated OA (LO-OOA) and more-oxidized oxygenated OA (MO-OOA) measured in urban areas of China. These
89 findings are aim to support for the estimation of these two urban lifestyle SOA in ambient air, conducting to the policy
90 formulation of pollution source control and health risk assessment of exposure to vehicle and cooking fumes.

91 **2. Material and Method**

92 **2.1 Experimental Setup**

93 The vehicle experiment was conducted from July to October in 2019, at Department of Automotive Engineering,
94 Tsinghua University. The cooking experiment was conducted from November 2019 to January 2020, at Langfang Branch,
95 Institute of Process Engineering, Chinese Academy of Sciences. The field study was deployed at the Institute of Atmospheric
96 Physics (IAP), Chinese Academy of Sciences (39°58'N; 116°22'E) in autumn and winter (Autumn: Oct. 1st, 2018 – Nov. 15th,
97 2018; Winter: Jan. 5th, 2019 – Jan. 31st, 2019) (Li et al., 2020a). The sample site is located in the south of Beitucheng West
98 Road and west of Beijing Chengde expressway in Beijing, which is a typical urban site affected by local emissions (Li et al.,



99 2020b).

100 The lab simulations of two urban lifestyle SOA were conducted with the same oxidation and measurement system. Tables
101 1-2 contain information of vehicle and cooking experiment conditions. The vehicle exhaust was emitted from a gasoline direct
102 engine (GDI) with China V gasoline (similar to Euro V) under three speeds (20, 40, 60 km/h), which represented the urban
103 road condition in China (Zhang et al., 2020a). For all experiments, the gasoline direct injection (GDI) engine ran in a single
104 room, its exhaust was drawn into pipeline and then entered the Go: PAM at a 30 fold dilution where aerosols and gases reacted
105 at a stable temperature and relative humidity. On the other hand, four kinds of domestic cuisines were cooked with liquefied
106 petroleum gas (LPG) in an iron wok, including deep-frying chicken, shallow-frying tofu, stir-frying cabbage and Kung Pao
107 chicken composed of cucumbers, peanuts and chicken. The cooking time and oil temperature were different due to the inherent
108 features of ingredients. For all experiments, the closed kitchen was full of fumes where the vision was blurred and the air was
109 choky after a long time of cooking process. Subsequently, the cooking fumes were drawn into pipeline from kitchen to lab
110 and then entered the Go: PAM at an 8 fold dilution where aerosols and gases reacted at a stable temperature and relative
111 humidity. Both vehicle and cooking fumes were diluted at a constant ratio by a Dekati Dilutor (e-Diluter, Dekati Ltd.). The
112 Go: PAM was able to produce high OH exposures using an ultraviolet lamp ($\lambda=254$ nm) in the presence of ozone and water
113 vapor, in order to simulate the photochemical oxidation in the atmosphere (Li et al., 2019a; Watne et al., 2018). Blank
114 experiments were separately designed in the presence of boiling water or dilution air under the same condition. The OA
115 concentrations of blank groups were far below those of experimental groups, which indicated the background values were
116 minor (Table S1). More details about experimental design and instruments can be found in Section S1.

117 **2.2 Measurements of the Gas and Particle Phase.**

118 Figure 1 presents the design of this lab simulation. The gases and aerosols were emitted from GDI room or kitchen, then
119 reacted and sampled in a lab. A high-resolution time-of-flight aerosol mass spectrometer (HR-ToF-AMS, Aerodyne Research
120 Inc.) was used to identify the chemical compositions of OA (Nash et al., 2006). Its time resolution was 2 min (precisely, 1
121 min for a mass sensitive V-mode, and 1 min for a high mass resolution W-mode). Two sets of scanning mobility particle sizers
122 (SMPS-1, Differential Mobility Analyzer, Electrostatic Classifier model 3080; Condensation Particle Counter model 3778;
123 SMPS-2, Differential Mobility Analyzer, Electrostatic Classifier model 3082; Condensation Particle Counter model 3772;
124 TSI Inc.) scanned every 2 min before and after Go: PAM individually to identify the size distribution and number
125 concentration of particles. The SMPS-1 determined the mass concentration of POA, while the SMPS-2 determined the mass
126 concentration of aged OA, and their mass difference could be regarded as the SOA. A SO₂ analyzer (Model 43i, Thermo
127 Electron Corp.) was used to measure the decay of SO₂ in offline adjustment. A CO₂ analyzer (Model 410i, Thermo Electron
128 Corp.) was used to reduce the CO₂ interference to organic fragments in mass spectra of HR-ToF-AMS. The particle densities
129 were measured through the determination of DMA-CPMA-CPC system (DMA-Differential Mobility Analyzer, Electrostatic
130 Classifier model 3080, TSI Inc.; CPMA- Centrifugal Particle Mass Analyzer, version 1.53, Cambustion Ltd.; CPC-
131 Condensation Particle Counter, Condensation Particle Counter model 3778, TSI Inc.). The POA (precisely, primary



132 Hydrocarbon-like OA, HOA, usually comes from vehicle exhaust; primary Cooking OA, COA) was regarded as the OA
133 measured before Go: PAM, or the OA measured after Go: PAM when the OH exposure was zero. The aged vehicle OA and
134 aged cooking OA were measured after Go: PAM under certain OH exposure. In order to prevent freshly warm gas from
135 condensing on the pipe wall, sampling pipes were equipped with heat insulation cotton and a temperature controller. Silicon
136 tubes were used to dry the emissions before they entered measuring instruments. Prior to each experiment, all pipelines and
137 the Go: PAM chamber were continuously flushed with purified dry air until the concentrations of gases and particles were
138 minimal.

139 **2.3 Data Analysis.**

140 **2.3.1 HR-ToF-AMS Data**

141 The SQUIRREL 1.57 and PIKA 1.16 written in IGOR (Wavemetrics Incorporation, USA) were used to analyze the HR-
142 ToF-AMS data including mass concentrations, elemental ratios, ion fragments and mass spectra. The ionization efficiency
143 (IE), relative ionization efficiency (RIE) and collection efficiency (CE) were determined individually before data processing.
144 The 300 nm ammonium nitrate particles were applied for converting the instrument signals to actual mass concentrations
145 (Jayne et al., 2000; Drewnick et al., 2005). A default value (1.4) of relative ionization efficiency (RIE) of OA was adopted.
146 Another synchronous SMPS-2 was used to correct the collection efficiency (CE) of HR-ToF-AMS by comparing their mass
147 concentrations (Gordon et al., 2014a). In order to separate the POA and SOA from aged OA, the mass spectra were resolved
148 by positive matrix factorization (PMF) analysis (Ulbrich et al., 2009).

149 **2.3.2 Determination and Evaluation of Oxidation Conditions in Go: PAM**

150 The Go: PAM conditions for vehicle and cooking experiments can be seen in Tables 3-4. The OH exposures and
151 corresponding photochemical ages in Go: PAM were calculated through an offline adjustment based on the decay of SO₂ (Lambe
152 et al., 2011). As shown in equation (1), K_{OH-SO₂} is the reaction rate constant of OH radical and SO₂ (9.0×10⁻¹³ molecule⁻¹·cm³·s⁻¹).
153 The SO_{2, f} and SO_{2, i} are the SO₂ concentrations (ppb) under the conditions of UV lamp on or off respectively. The
154 photochemical age (days) can be calculated in equation (2) when assuming the OH concentration is 1.5×10⁶ molecules·cm⁻³
155 in the atmosphere (Mao et al., 2009).

$$156 \quad OH \text{ exposure} = \frac{-1}{K_{OH-SO_2}} \times \ln\left(\frac{SO_{2,f}}{SO_{2,i}}\right) \quad (1)$$

$$157 \quad Photochemical \text{ age} = \frac{OH \text{ exposure}}{24 \times 3600 \times 1.5 \times 10^6} \quad (2)$$

158 Except for the off-line calibration based on the decay of SO₂, a flow reactor exposure estimator was also used in this
159 study (Peng et al., 2016). The OH exposures calculated by both methods showed a good correlation (Figure S1&S2). This
160 estimator could also evaluate the potential non-OH reactions in flow reactor such as the photolysis of VOCs, the reactions
161 with O(¹D), O(³P) and O₃. Our results showed that non-OH reactions were not significant except for the photolysis of
162 acetylacetone. But there is no acetylacetone from vehicle exhaust or cooking emission according to our measurements and
163 previous studies. The acetylacetone was usually considered as a kind of VOCs emitted from industrial production (Ji et al.,



164 2020). Therefore, its potential photolysis wouldn't take place during our cooking conditions, and OH reactions still played
165 the dominant role. Overall, our Go: PAM could reasonably simulate the oxidation process of cooking OA in ambient.

166 Furthermore, the external OH reactivity and OH exposure were both influenced by external OH reactants, such as NO_x
167 and VOCs during experiments. The NO_x concentration was measured by a NO-NO₂-NO_x Analyzer (Model 42i, Thermo
168 Electron Corporation, USA). As for VOCs, we have divided them into 5 types including alkane, alkene, aromatic, O-VOCs
169 (Oxidized VOCs, mainly included aldehyde and ketone) and X-VOCs (halogenated-VOCs) using the measurement of GC-
170 MS (Gas Chromatography-Mass Spectrometry, GC-7890, MS-5977, Agilent Technologies Inc). The compounds with
171 relatively high proportion were regarded as surrogate species for each type of VOCs. The total concentrations of VOCs were
172 determined by a portable TVOC Analyzer (PGM-7340, RAE SYSTEMS). The external OH reactivities for different vehicle
173 experiments (10.4~20.2 s⁻¹) were all comparable to that of off-line calibration result (15.8 s⁻¹), and the external OH reactivities
174 for different cooking experiments (21.7~25.7 s⁻¹) were also comparable to that of off-line calibration result (24.0 s⁻¹). Besides,
175 the ratio of OH exposure calculated by the estimator to that calculated by the decay of SO₂ ranged from 83% to 119% for
176 vehicle experiments and 97% to 111% for cooking experiments, which means that our off-line OH exposure could be a
177 representative value to all experiments. The mixing and wall loss conditions have already met our experiment needs. Detailed
178 tests about mixing condition and wall loss of the Go: PAM have been conducted in previous work according to Li et al. (Li et
179 al., 2019a) and Watne et al. (Watne et al., 2018), which could be found in Figure S3(a). In this study, we still corrected the wall
180 loss of particle in each size bin measured by two synchronous SMPS (two SMPS run before and after Go: PAM respectively).

181 **3. Result and Discussion**

182 **3.1 Formation Potential of the Urban Lifestyle SOA.**

183 As Figure 2 shows, the mass growth potentials of two urban lifestyle SOA were quite different. Although their SOA/POA
184 mass ratios both increased gradually through functionalization reactions and finally reached the peak after 2-3 days of
185 equivalent photochemical age (Kroll et al., 2009), the overall SOA mass growth potentials of vehicle SOA were far larger
186 than those of cooking SOA. When the equivalent photochemical age was near 2 days (1.7 days), the mass growth potentials
187 of vehicle SOA ranged from 83 to 150. In contrast, the mass growth potentials of cooking SOA only ranged from 1.8 to 3.2
188 at about 2.1 days. Even if there was still a slight growth trend for cooking SOA at the highest OH exposure, it surely exhibited
189 a much weaker mass growth potential on the whole compared with that of vehicle SOA. This significant distinction indicated
190 that the vehicle exhaust may contribute abundant SOA and relatively fewer POA, while cooking emission may produce
191 moderate POA and SOA in the atmosphere, which could attribute to their different types of gaseous precursors. For instance,
192 vehicle tended to generate large amounts of aromatics and cycloalkanes, which showed high rate constants of reaction with
193 OH and would lead to large SOA yields (Zhang et al., 2020a; Atkinson and Arey, 2003; Peng et al., 2017). By contrast, cooking
194 tended to emit much more unsaturated fatty acids that were tough to be oxidized even under high OH exposures (Zeng et al.,
195 2020; Nah et al., 2013). Interestingly, a similar phenomenon had been observed from an OFR simulation in the urban roadside
196 of Hongkong where potential SOA from motor vehicle exhaust was much larger than primary HOA, while potential SOA



197 from cooking emission was comparable to primary COA (Liu et al., 2019).

198 **3.2 Formation Pathway of the Urban Lifestyle SOA.**

199 As Figure 3 shows, the O:C molar ratios (O/C) of two urban lifestyle SOA were quite different. Although their oxidation
200 degrees both increased gradually and finally reached the peak after 2-3 days of equivalent photochemical age, the O/C values
201 of vehicle SOA were far larger than those of cooking SOA. When the equivalent photochemical age was 0.6 day, the O/C of
202 vehicle SOA was 0.4-0.5, resembling a kind of LO-OOA in ambient air. When the equivalent photochemical age was near 2
203 days (1.7 days), the O/C of vehicle SOA could reach 0.6, which was almost like a type of MO-OOA in the atmosphere. In
204 contrast, the O/C of cooking SOA only rose to 0.4 at 2.1 days, similar to a kind of LO-OOA. These distinct features of O/C
205 suggested that vehicle SOA was divided into LO-OOA and MO-OOA under different oxidation conditions, while the cooking
206 SOA was only composed of LO-OOA. This difference was probably related to their precursors. For example, vehicle emitted
207 large amounts of aromatics such as toluene, producing abundant SOA with a higher state of oxidation (Zhang et al.,
208 2020a;Suarez-Bertoa et al., 2015;Nordin et al., 2013;Liu et al., 2015;Deng et al., 2017). On the contrary, cooking generated
209 many unsaturated fatty acids such as oleic acid, which would remain unreacted under high OH exposures and thus retained
210 some features of fresh POA (Nah et al., 2013;Klein et al., 2016).

211 Figure 4 illustrates diverse oxidation pathways of various sources of OA in a Van Krevelen diagram (Heald et al.,
212 2010;Ng et al., 2011;Presto et al., 2014). The cooking groups fell along a line with a slope of -0.10 implying an
213 alcohol/peroxide pathway in forming SOA, while the vehicle groups fell along a line with a slope of -0.55 implying an
214 oxidation pathway between alcohol/peroxide and carboxylic acid reaction. Additionally, these two secondary evolution
215 properties are both different from those of biomass burning OA (slope \approx -0.6) (Lim et al., 2019) and ambient OA (slope \approx -1 to
216 -0.5) (Heald et al., 2010;Hu et al., 2017;Ng et al., 2011), indicating that these two urban lifestyles SOA may undergo distinct
217 oxidation pathways.

218 **3.3 Characteristics in Mass Spectra of the Urban Lifestyle SOA.**

219 As shown in Figure 5, m/z 43 (f_{43}) vs. m/z 44 (f_{44}) plot has been widely adopted to represent the oxidation process of
220 OA (Ng et al., 2010;Hennigan et al., 2011). Generally, f_{43} and f_{44} derive from oxygen-containing fragments, the former comes
221 from less oxidized components while the latter comes from more oxidized ones. The datasets of vehicle and cooking groups
222 apparently fell along in different regions and showed different variations in the plot. Almost all cooking OA displayed
223 relatively lower f_{44} and higher f_{43} , and its f_{43} and f_{44} both increased slightly with the growing OH exposure, eventually
224 distributing in the LO-OOA region. In contrast, all vehicle OA displayed moderate f_{43} and abundant f_{44} , and only its f_{44}
225 showed an obvious souring with the growing OH exposure, initially distributing in the LO-OOA region but finally spreading
226 near the MO-OOA region. These distinct evolutions of oxygen-containing fragments for two urban lifestyle SOA inferred
227 their intrinsic oxidation pathways and precursors. Vehicle might emit more easily oxidized aromatics, e.g. toluene and xylene,
228 while cooking might produce more hardly oxidized fatty acids such as palmitic acid and octadecanoic acid (Zhao et al.,
229 2007;Reyes-Villegas et al., 2018;Schauer et al., 2002;Zeng et al., 2020;Deng et al., 2017;Gordon et al., 2014b;Nah et al.,



230 2013;Zhang et al., 2020a).

231 Figure 6 and Table 5 depict mass spectra and prominent peaks of aged OA from two urban lifestyle sources which could
232 be used to deduce their inherent properties (Zhang et al., 2005;Kaltsonoudis et al., 2017;Liu et al., 2018;Chirico et al.,
233 2010;Nordin et al., 2013;Zhang et al., 2020b). The maximum SOA mass growth potentials of aged cooking SOA only ranged
234 from 1.9-3.2 implying a mixture of POA and SOA, so its mass spectra needed to be deeply resolved by PMF in order to
235 separate the POA and SOA (precisely, a kind of LO-OOA). However, those mass growth potentials of aged vehicle OA were
236 extremely high, suggesting that it was fully oxidized and almost composed of SOA. According to the O/C ratios, the vehicle
237 SOA under 0.6 day of photochemical age was defined as vehicle LO-OOA, while that under 2.9 days was regarded as vehicle
238 MO-OOA.

239 For average vehicle LO-OOA mass spectra, the prominent peaks were m/z 43 ($f_{43}=0.133$), 44 ($f_{44}=0.077$), 29 ($f_{29}=0.076$),
240 28 ($f_{28}=0.066$), 41 ($f_{41}=0.051$), 55 ($f_{55}=0.043$) dominated by $C_2H_3O^+$, $C_3H_7^+$, CO_2^+ , CHO^+ , $C_2H_5^+$, CO^+ , $C_3H_5^+$, $C_3H_3O^+$ and
241 $C_4H_7^+$ respectively, while the prominent peaks of average vehicle MO-OOA were m/z 44 ($f_{43}=0.146$), 28 ($f_{44}=0.134$), 43
242 ($f_{43}=0.117$), 29 ($f_{29}=0.071$), 45 ($f_{45}=0.032$), 27 ($f_{27}=0.031$) dominated by CO_2^+ , CO^+ , $C_2H_3O^+$, CHO^+ , $C_2H_5^+$, CHO_2^+ , $C_2H_5O^+$
243 and $C_2H_3^+$ respectively. Compared with vehicle SOA mass spectra from other studies (Table 5), our average GDI SOA (LO-
244 OOA and MO-OOA) illustrated more abundances of oxygen-containing ions than those of Gasoline SOA and Diesel SOA
245 simulated by a smog chamber with lower OH exposures (Chirico et al., 2010;Nordin et al., 2013).

246 For average cooking LO-OOA, it was less oxidized than those from vehicle groups, whose prominent peaks were m/z
247 43 ($f_{43}=0.097$), 44 ($f_{44}=0.065$), 29 ($f_{29}=0.065$), 41 ($f_{41}=0.058$), 55 ($f_{55}=0.056$), 28 ($f_{28}=0.053$) dominated by $C_2H_3O^+$, $C_3H_7^+$,
248 CO_2^+ , CHO^+ , $C_2H_5^+$, $C_3H_5^+$, $C_3H_3O^+$, $C_4H_7^+$ and CO^+ respectively. Compared with other cooking SOA mass spectra (Table
249 5), our average cooking LO-OOA had similar peaks with heated oil SOA, but was different from that meat charbroiling SOA
250 which displayed much more hydrocarbon-like features (Liu et al., 2018;Kaltsonoudis et al., 2017).

251 3.4 Potential Chemical Evolution of Urban Lifestyle SOA in the Atmosphere.

252 The AMS mass spectra indicated that the chemical evolution of urban lifestyle SOA in the Go: PAM might provide new
253 insights and references on those of ambient SOA observed in the atmosphere. Figure 7 plots the correlation coefficients
254 between the lab aged OA and ambient PMF-OA factors with growing photochemical ages (Li et al., 2020a). Table 6 exhibits
255 correlations of mass spectra between lab results and ambient PMF factors, where the aged lab cooking OA was divided into
256 POA and LO-OOA while the lab vehicle OA was divided into LO-OOA and MO-OOA.

257 For aged GDI OA in Figure 7, its average mass spectra still remained some ambient HOA features (pearson $r=0.80$)
258 under low photochemical age of 0.6 day with moderate hydrocarbon-like ions such as m/z 41 and 55, but it had already
259 reached the same oxidation degree of ambient LO-OOA (pearson $r=0.81$) with high O/C (0.46) and f_{43} (0.133). After aging
260 in the Go: PAM, aged OA might finally become a kind of ambient MO-OOA (pearson $r=0.97$) at 5.1 days of photochemical
261 age. This evolution of GDI OA (from HOA to LO-OOA to MO-OOA) was similar to the result of a previous vehicle OA
262 simulation (from HOA to SV-OOA to LV-OOA) (Tkacik et al., 2014).



263 For aged cooking OA in Figure 7, although its correlations with ambient LO-OOA increased gradually from 0.56 to 0.73
264 along with the growing photochemical ages, its correlations with ambient COA kept a high level all the time (pearson $r > 0.81$)
265 implying a mixture of POA and SOA due to some hardly oxidized compounds emitted from the cooking process. Therefore,
266 it is necessary to resolve aged cooking OA mass spectra deeply by PMF (Figures S4-S11) and then compared its lab PMF
267 results with ambient PMF factors. As Table 6 shows, the lab cooking POA was similar to ambient COA (pearson $r = 0.86$) but
268 less likely to LO-OOA (pearson $r = 0.46$) or MO-OOA (pearson $r = 0.39$). By contrast, the lab cooking LO-OOA displayed
269 many more ambient LO-OOA features (pearson $r = 0.76$) and relatively fewer ambient COA characteristics than lab cooking
270 POA did. In short, these comparisons between lab and ambient results revealed that organics from these two urban lifestyle
271 sources might eventually form different SOA types in the real atmosphere.

272 4. Conclusion

273 In the present work, we define two urban lifestyle SOA in details and investigate their mass growth potentials, formation
274 pathways, mass spectra, and chemical evolutions comprehensively. At about 2 days of equivalent photochemical age, the
275 SOA/POA mass ratios of vehicle groups (107) were 44 times larger than those of cooking groups (2.38), and the O: C molar
276 ratios of vehicle groups (0.66) was about 2 times large as those of cooking groups (0.34). Besides, both vehicle and cooking
277 groups underwent alcohol/peroxide pathway to form LO-OOA, and the vehicle groups extra underwent carboxylic acid
278 pathway to form part of MO-OOA. Furthermore, the characteristic mass spectra of these two urban lifestyle SOA could
279 provide necessary references to estimate their mass fractions in ambient air, through a multilinear engine model (ME-2)
280 (Canonaco et al., 2013; Qin et al., 2017). This application would reduce the large gaps of total atmospheric contributions and
281 relevant environment effects for urban SOA, although remaining several uncertainties on SOA mass spectra due to missing
282 complex mixture conditions in the Go: PAM.

283 Although strict policies have been implemented to reduce primary particulate matter (PM) in urban areas. However,
284 secondary PM especially for the abundant and complicated SOA, is difficult to be restricted (Wu et al., 2017; Li et al., 2018).
285 According to our results, on the one hand, vehicle SOA might be a mixture of both LO-OOA and MO-OOA with high
286 secondary formation potential, so it would be better not only filter out the exhaust PM with Gasoline Particulate Filter (GPF),
287 but also reduce the gaseous precursors in order to restrict the secondary formation. On the other hand, cooking SOA might be
288 a kind of LO-OOA with relatively low secondary formation potential, so it could be enough to remove the gas and particle
289 emissions at the same level. In the future, these two urban lifestyle SOA may present increasing contributions in urban areas
290 especially in megacities with growing atmospheric oxidants (Li et al., 2019b; Wang et al., 2017; Li et al., 2020a; Li et al., 2020b),
291 but their investigations and further managements are far from sufficient, making it possible to become a greatly meaningful
292 research focus.

293

294

295



296 *Data availability.* The data provided in this paper can be obtained from the author upon request (minhu@pku.edu.cn).

297

298 *Supplement.* An independent supplement document is available.

299

300 *Authorship contributions.* Zirui Zhang: Investigation, Data curation, Methodology, Formal analysis, Writing - original draft,
301 Writing - review & editing. Wenfei Zhu: Investigation, Data curation, Methodology, Formal analysis, Writing - review &
302 editing. Min Hu: Project administration, Supervision, Funding acquisition, Writing - review & editing. Kefan Liu:
303 Investigation, Data curation, Formal analysis. Hui Wang: Investigation, Data curation. Rongzhi Tang Investigation, Data
304 curation. Ruizhe Shen: Investigation, Data curation. Ying Yu: Investigation, Data curation. Rui Tan: Investigation, Data
305 curation. Kai Song: Investigation, Data curation. Yuanju Li: Investigation, Data curation. Wenbin Zhang: Investigation, Data
306 curation. Zhou Zhang: Investigation, Data curation. Hongming Xu: Data curation. Shijin Shuai: Data curation. Shuangde Li:
307 Data curation. Yunfa Chen: Data curation. Jiayun Li: Data curation. Yuesi Wang: Data curation. Song Guo: Project
308 administration, Funding acquisition, Writing - review & editing.

309 Note: Zirui Zhang and Wenfei Zhu contributed equally to this work.

310

311 *Competing interests.* The authors declare that they have no known competing financial interests or personal relationships that
312 could have appeared to influence the work reported in this paper.

313

314 *Acknowledgements.* Thanks to all authors from PKU who had directly participate in the main lab simulation.
315 Thanks to all authors from THU and CAS who had provide necessary experiment sites, instruments and data
316 supports.

317

318 *Financial support.* The research has been supported by the National Key R&D Program of China (2016YFC0202000), the
319 National Natural Science Foundation of China (51636003, 91844301, 41977179, and 21677002), Beijing Municipal Science
320 and Technology Commission (Z201100008220011), Open Research Fund of State Key Laboratory of Multiphase Complex
321 Systems (MPCS-2019-D-09), and China Postdoctoral Science Foundation (2020M680242).

322

323

324

325

326

327

328



329 REFERENCES

- 330 Alanen, J., Simonen, P., Saarikoski, S., Timonen, H., Kangasniemi, O., Saukko, E., Hillamo, R., Lehtoranta, K., Murtonen, T.,
331 Vesala, H., Keskinen, J., and Rönkkö, T.: Comparison of primary and secondary particle formation from natural gas engine
332 exhaust and of their volatility characteristics, *Atmospheric Chemistry and Physics*, 17, 8739-8755, 10.5194/acp-17-8739-
333 2017, 2017.
- 334 Allan, J. D., Williams, P. I., Morgan, W. T., Martin, C. L., Flynn, M. J., Lee, J., Nemitz, E., Phillips, G. J., Gallagher, M. W., and Coe,
335 H.: Contributions from transport, solid fuel burning and cooking to primary organic aerosols in two UK cities, *Atmospheric*
336 *Chemistry And Physics*, 10, 647-668, 10.5194/acp-10-647-2010, 2010.
- 337 An, Z., Huang, R. J., Zhang, R., Tie, X., Li, G., Cao, J., Zhou, W., Shi, Z., Han, Y., Gu, Z., and Ji, Y.: Severe haze in northern China:
338 A synergy of anthropogenic emissions and atmospheric processes, *Proceedings of the National Academy of Sciences of the*
339 *United States of America*, 116, 8657-8666, 10.1073/pnas.1900125116, 2019.
- 340 Atkinson, R., and Arey, J.: Atmospheric degradation of volatile organic compounds, *Chemical reviews*, 103, 4605-4638,
341 10.1021/cr0206420, 2003.
- 342 Canonaco, F., Crippa, M., Slowik, J. G., Baltensperger, U., and Prévôt, A. S. H.: SoFi, an IGOR-based interface for the efficient
343 use of the generalized multilinear engine (ME-2) for the source apportionment: ME-2 application to aerosol mass
344 spectrometer data, *Atmospheric Measurement Techniques*, 6, 3649-3661, 10.5194/amt-6-3649-2013, 2013.
- 345 Chan, C. K., and Yao, X.: Air pollution in mega cities in China, *Atmospheric Environment*, 42, 1-42,
346 10.1016/j.atmosenv.2007.09.003, 2008.
- 347 Chirico, R., DeCarlo, P. F., Heringa, M. F., Tritscher, T., Richter, R., Prevot, A. S. H., Dommen, J., Weingartner, E., Wehrle, G.,
348 Gysel, M., Laborde, M., and Baltensperger, U.: Impact of aftertreatment devices on primary emissions and secondary organic
349 aerosol formation potential from in-use diesel vehicles: results from smog chamber experiments, *Atmospheric Chemistry*
350 *And Physics*, 10, 11545-11563, 10.5194/acp-10-11545-2010, 2010.
- 351 Crippa, M., DeCarlo, P. F., Slowik, J. G., Mohr, C., Heringa, M. F., Chirico, R., Poulain, L., Freutel, F., Sciare, J., Cozic, J., Di Marco,
352 C. F., Elsasser, M., Nicolas, J. B., Marchand, N., Abidi, E., Wiedensohler, A., Drewnick, F., Schneider, J., Borrmann, S., Nemitz,
353 E., Zimmermann, R., Jaffrezo, J. L., Prevot, A. S. H., and Baltensperger, U.: Wintertime aerosol chemical composition and
354 source apportionment of the organic fraction in the metropolitan area of Paris, *Atmospheric Chemistry And Physics*, 13,
355 961-981, 10.5194/acp-13-961-2013, 2013.
- 356 de Gouw, J. A., Brock, C. A., Atlas, E. L., Bates, T. S., Fehsenfeld, F. C., Goldan, P. D., Holloway, J. S., Kuster, W. C., Lerner, B.
357 M., Matthew, B. M., Middlebrook, A. M., Onasch, T. B., Peltier, R. E., Quinn, P. K., Senff, C. J., Stohl, A., Sullivan, A. P., Trainer,
358 M., Warneke, C., Weber, R. J., and Williams, E. J.: Sources of particulate matter in the northeastern United States in summer:
359 1. Direct emissions and secondary formation of organic matter in urban plumes, *Journal of Geophysical Research*, 113,
360 10.1029/2007jd009243, 2008.
- 361 Deng, W., Hu, Q., Liu, T., Wang, X., Zhang, Y., Song, W., Sun, Y., Bi, X., Yu, J., Yang, W., Huang, X., Zhang, Z., Huang, Z., He,
362 Q., Mellouki, A., and George, C.: Primary particulate emissions and secondary organic aerosol (SOA) formation from idling
363 diesel vehicle exhaust in China, *The Science of the total environment*, 593-594, 462-469, 10.1016/j.scitotenv.2017.03.088,
364 2017.
- 365 Deng, W., Fang, Z., Wang, Z., Zhu, M., Zhang, Y., Tang, M., Song, W., Lowther, S., Huang, Z., Jones, K., Peng, P., and Wang,
366 X.: Primary emissions and secondary organic aerosol formation from in-use diesel vehicle exhaust: Comparison between
367 idling and cruise mode, *The Science of the total environment*, 699, 134357, 10.1016/j.scitotenv.2019.134357, 2020.
- 368 Donahue, N. M., Robinson, A. L., and Pandis, S. N.: Atmospheric organic particulate matter: From smoke to secondary
369 organic aerosol, *Atmospheric Environment*, 43, 94-106, 10.1016/j.atmosenv.2008.09.055, 2009.
- 370 Drewnick, F., Hings, S. S., DeCarlo, P., Jayne, J. T., Gonin, M., Fuhrer, K., Weimer, S., Jimenez, J. L., Demerjian, K. L., Borrmann,
371 S., and Worsnop, D. R.: A New Time-of-Flight Aerosol Mass Spectrometer (TOF-AMS)—Instrument Description and First
372 Field Deployment, *Aerosol Science and Technology*, 39, 637-658, 10.1080/02786820500182040, 2005.
- 373 Du, Z., Hu, M., Peng, J., Zhang, W., Zheng, J., Gu, F., Qin, Y., Yang, Y., Li, M., Wu, Y., Shao, M., and Shuai, S.: Comparison of
374 primary aerosol emission and secondary aerosol formation from gasoline direct injection and port fuel injection vehicles,
375 *Atmospheric Chemistry and Physics*, 18, 9011-9023, 10.5194/acp-18-9011-2018, 2018.
- 376 Esmaeilirad, S., and Hosseini, V.: Modeling the formation of traditional and non-traditional secondary organic aerosols from



- 377 in-use, on-road gasoline and diesel vehicles exhaust, *Journal of Aerosol Science*, 124, 68–82, 10.1016/j.jaerosci.2018.07.003,
378 2018.
- 379 Ge, X., Setyan, A., Sun, Y., and Zhang, Q.: Primary and secondary organic aerosols in Fresno, California during wintertime:
380 Results from high resolution aerosol mass spectrometry, *Journal of Geophysical Research: Atmospheres*, 117, n/a–n/a,
381 10.1029/2012jd018026, 2012.
- 382 Gordon, T. D., Tkacik, D. S., Presto, A. A., Zhang, M., Jathar, S. H., Nguyen, N. T., Massetti, J., Truong, T., Cicero-Fernandez,
383 P., Maddox, C., Rieger, P., Chattopadhyay, S., Maldonado, H., Maricq, M. M., and Robinson, A. L.: Primary gas- and particle-
384 phase emissions and secondary organic aerosol production from gasoline and diesel off-road engines, *Environmental
385 science & technology*, 47, 14137–14146, 10.1021/es403556e, 2013.
- 386 Gordon, T. D., Presto, A. A., May, A. A., Nguyen, N. T., Lipsky, E. M., Donahue, N. M., Gutierrez, A., Zhang, M., Maddox, C.,
387 Rieger, P., Chattopadhyay, S., Maldonado, H., Maricq, M. M., and Robinson, A. L.: Secondary organic aerosol formation
388 exceeds primary particulate matter emissions for light-duty gasoline vehicles, *Atmospheric Chemistry and Physics*, 14, 4661–
389 4678, 10.5194/acp-14-4661-2014, 2014a.
- 390 Gordon, T. D., Presto, A. A., Nguyen, N. T., Robertson, W. H., Na, K., Sahay, K. N., Zhang, M., Maddox, C., Rieger, P.,
391 Chattopadhyay, S., Maldonado, H., Maricq, M. M., and Robinson, A. L.: Secondary organic aerosol production from diesel
392 vehicle exhaust: impact of aftertreatment, fuel chemistry and driving cycle, *Atmospheric Chemistry and Physics*, 14, 4643–
393 4659, 10.5194/acp-14-4643-2014, 2014b.
- 394 Guo, S., Hu, M., Guo, Q., Zhang, X., Zheng, M., Zheng, J., Chang, C. C., Schauer, J. J., and Zhang, R.: Primary sources and
395 secondary formation of organic aerosols in Beijing, China, *Environmental science & technology*, 46, 9846–9853,
396 10.1021/es2042564, 2012.
- 397 Guo, S., Hu, M., Guo, Q., Zhang, X., Schauer, J. J., and Zhang, R.: Quantitative evaluation of emission controls on primary
398 and secondary organic aerosol sources during Beijing 2008 Olympics, *Atmospheric Chemistry and Physics*, 13, 8303–8314,
399 10.5194/acp-13-8303-2013, 2013.
- 400 Guo, S., Hu, M., Zamora, M. L., Peng, J. F., Shang, D. J., Zheng, J., Du, Z. F., Wu, Z., Shao, M., Zeng, L. M., Molina, M. J., and
401 Zhang, R. Y.: Elucidating severe urban haze formation in China, *Proceedings of the National Academy of Sciences of the
402 United States of America*, 111, 17373–17378, 10.1073/pnas.1419604111, 2014.
- 403 Guo, S., Hu, M., Peng, J. F., Wu, Z. J., Zamora, M. L., Shang, D. J., Du, Z. F., Zheng, J., Fang, X., Tang, R. Z., Wu, Y. S., Zeng, L.
404 M., Shuai, S. J., Zhang, W. B., Wang, Y., Ji, Y. M., Li, Y. X., Zhang, A. L., Wang, W. G., Zhang, F., Zhao, J. Y., Gong, X. L., Wang,
405 C. Y., Molina, M. J., and Zhang, R. Y.: Remarkable nucleation and growth of ultrafine particles from vehicular exhaust,
406 *Proceedings of the National Academy of Sciences of the United States of America*, 117, 3427–3432,
407 10.1073/pnas.1916366117, 2020.
- 408 Hallquist, M., Munthe, J., Hu, M., Wang, T., Chan, C. K., Gao, J., Boman, J., Guo, S., Hallquist, A. M., Mellqvist, J., Moldanova,
409 J., Pathak, R. K., Pettersson, J. B. C., Pleijel, H., Simpson, D., and Thynell, M.: Photochemical smog in China: scientific challenges
410 and implications for air-quality policies, *Natl. Sci. Rev.*, 3, 401–403, 10.1093/nsr/nww080, 2016.
- 411 Hayes, P. L., Carlton, A. G., Baker, K. R., Ahmadov, R., Washenfelder, R. A., Alvarez, S., Rappenglück, B., Gilman, J. B., Kuster,
412 W. C., de Gouw, J. A., Zotter, P., Prévôt, A. S. H., Szidat, S., Kleindienst, T. E., Offenberg, J. H., Ma, P. K., and Jimenez, J. L.:
413 Modeling the formation and aging of secondary organic aerosols in Los Angeles during CalNex 2010, *Atmospheric
414 Chemistry and Physics*, 15, 5773–5801, 10.5194/acp-15-5773-2015, 2015.
- 415 Heald, C. L., Kroll, J. H., Jimenez, J. L., Docherty, K. S., DeCarlo, P. F., Aiken, A. C., Chen, Q., Martin, S. T., Farmer, D. K., and
416 Artaxo, P.: A simplified description of the evolution of organic aerosol composition in the atmosphere, *Geophysical Research
417 Letters*, 37, 10.1029/2010gl042737, 2010.
- 418 Hennigan, C. J., Miracolo, M. A., Engelhart, G. J., May, A. A., Presto, A. A., Lee, T., Sullivan, A. P., McMeeking, G. R., Coe, H.,
419 Wold, C. E., Hao, W. M., Gilman, J. B., Kuster, W. C., de Gouw, J., Schichtel, B. A., Collett, J. L., Kreidenweis, S. M., and Robinson,
420 A. L.: Chemical and physical transformations of organic aerosol from the photo-oxidation of open biomass burning
421 emissions in an environmental chamber, *Atmospheric Chemistry and Physics*, 11, 7669–7686, 10.5194/acp-11-7669-2011,
422 2011.
- 423 Hu, M., Guo, S., Peng, J. F., and Wu, Z. J.: Insight into characteristics and sources of PM_{2.5} in the Beijing–Tianjin–Hebei region,
424 *China, Natl. Sci. Rev.*, 2, 257–258, 10.1093/nsr/nww003, 2015.
- 425 Hu, W., Hu, M., Hu, W. W., Zheng, J., Chen, C., Wu, Y. S., and Guo, S.: Seasonal variations in high time-resolved chemical



- 426 compositions, sources, and evolution of atmospheric submicron aerosols in the megacity Beijing, *Atmospheric Chemistry*
427 *And Physics*, 17, 9979-10000, 10.5194/acp-17-9979-2017, 2017.
- 428 Jayne, J. T., Leard, D. C., Zhang, X., Davidovits, P., Smith, K. A., Kolb, C. E., and Worsnop, D. R.: Development of an Aerosol
429 Mass Spectrometer for Size and Composition Analysis of Submicron Particles, *Aerosol Science and Technology*, 33, 49-70,
430 10.1080/027868200410840, 2000.
- 431 Ji, Y., Qin, D., Zheng, J., Shi, Q., Wang, J., Lin, Q., Chen, J., Gao, Y., Li, G., and An, T.: Mechanism of the atmospheric chemical
432 transformation of acetylacetone and its implications in night-time second organic aerosol formation, *The Science of the*
433 *total environment*, 720, 137610, 10.1016/j.scitotenv.2020.137610, 2020.
- 434 Jimenez, J. L., Canagaratna, M. R., Donahue, N. M., Prevot, A. S., Zhang, Q., Kroll, J. H., DeCarlo, P. F., Allan, J. D., Coe, H., Ng,
435 N. L., Aiken, A. C., Docherty, K. S., Ulbrich, I. M., Grieshop, A. P., Robinson, A. L., Duplissy, J., Smith, J. D., Wilson, K. R., Lanz,
436 V. A., Hueglin, C., Sun, Y. L., Tian, J., Laaksonen, A., Raatikainen, T., Rautiainen, J., Vaattovaara, P., Ehn, M., Kulmala, M.,
437 Tomlinson, J. M., Collins, D. R., Cubison, M. J., Dunlea, E. J., Huffman, J. A., Onasch, T. B., Alfarra, M. R., Williams, P. I., Bower,
438 K., Kondo, Y., Schneider, J., Drewnick, F., Borrmann, S., Weimer, S., Demerjian, K., Salcedo, D., Cottrell, L., Griffin, R., Takami,
439 A., Miyoshi, T., Hatakeyama, S., Shimono, A., Sun, J. Y., Zhang, Y. M., Dzepina, K., Kimmel, J. R., Sueper, D., Jayne, J. T.,
440 Herndon, S. C., Trimborn, A. M., Williams, L. R., Wood, E. C., Middlebrook, A. M., Kolb, C. E., Baltensperger, U., and Worsnop,
441 D. R.: Evolution of organic aerosols in the atmosphere, *Science*, 326, 1525-1529, 10.1126/science.1180353, 2009.
- 442 Kaltsonoudis, C., Kostenidou, E., Louvaris, E., Psychoudaki, M., Tsiligiannis, E., Florou, K., Liangou, A., and Pandis, S. N.:
443 Characterization of fresh and aged organic aerosol emissions from meat charbroiling, *Atmospheric Chemistry and Physics*,
444 17, 7143-7155, 10.5194/acp-17-7143-2017, 2017.
- 445 Katragadda, H. R., Fullana, A., Sidhu, S., and Carbonell-Barrachina, Á. A.: Emissions of volatile aldehydes from heated cooking
446 oils, *Food Chemistry*, 120, 59-65, 10.1016/j.foodchem.2009.09.070, 2010.
- 447 Kim, C., Gao, Y. T., Xiang, Y. B., Barone-Adesi, F., Zhang, Y., Hosgood, H. D., Ma, S., Shu, X. O., Ji, B. T., Chow, W. H., Seow,
448 W. J., Bassig, B., Cai, Q., Zheng, W., Rothman, N., and Lan, Q.: Home kitchen ventilation, cooking fuels, and lung cancer risk
449 in a prospective cohort of never smoking women in Shanghai, China, *International journal of cancer*, 136, 632-638,
450 10.1002/ijc.29020, 2015.
- 451 Klein, F., Platt, S. M., Farren, N. J., Detournay, A., Bruns, E. A., Bozzetti, C., Daellenbach, K. R., Kilic, D., Kumar, N. K., Pieber, S.
452 M., Slowik, J. G., Temime-Roussel, B., Marchand, N., Hamilton, J. F., Baltensperger, U., Prevot, A. S., and El Haddad, I.:
453 Characterization of Gas-Phase Organics Using Proton Transfer Reaction Time-of-Flight Mass Spectrometry: Cooking
454 Emissions, *Environmental science & technology*, 50, 1243-1250, 10.1021/acs.est.5b04618, 2016.
- 455 Kleinman, L. I., Springston, S. R., Daum, P. H., Lee, Y. N., Nunnermacker, L. J., Senum, G. I., Wang, J., Weinstein-Lloyd, J.,
456 Alexander, M. L., Hubbe, J., Ortega, J., Canagaratna, M. R., and Jayne, J.: The time evolution of aerosol composition over the
457 Mexico City plateau, *Atmospheric Chemistry And Physics*, 8, 1559-1575, 10.5194/acp-8-1559-2008, 2008.
- 458 Kroll, J. H., Smith, J. D., Che, D. L., Kessler, S. H., Worsnop, D. R., and Wilson, K. R.: Measurement of fragmentation and
459 functionalization pathways in the heterogeneous oxidation of oxidized organic aerosol, *Phys. Chem. Chem. Phys.*, 11, 8005-
460 8014, 10.1039/b905289e, 2009.
- 461 Lambe, A. T., Ahern, A. T., Williams, L. R., Slowik, J. G., Wong, J. P. S., Abbatt, J. P. D., Brune, W. H., Ng, N. L., Wright, J. P.,
462 Croasdale, D. R., Worsnop, D. R., Davidovits, P., and Onasch, T. B.: Characterization of aerosol photooxidation flow reactors:
463 heterogeneous oxidation, secondary organic aerosol formation and cloud condensation nuclei activity measurements,
464 *Atmospheric Measurement Techniques*, 4, 445-461, 10.5194/amt-4-445-2011, 2011.
- 465 Lee, B. P., Li, Y. J., Yu, J. Z., Louie, P. K. K., and Chan, C. K.: Characteristics of submicron particulate matter at the urban
466 roadside in downtown Hong Kong-Overview of 4 months of continuous high-resolution aerosol mass spectrometer
467 measurements, *Journal of Geophysical Research: Atmospheres*, 120, 7040-7058, 10.1002/2015jd023311, 2015.
- 468 Li, J., Li, X.-B., Li, B., and Peng, Z.-R.: The Effect of Nonlocal Vehicle Restriction Policy on Air Quality in Shanghai, *Atmosphere*,
469 9, 299, 10.3390/atmos9080299, 2018.
- 470 Li, J., Liu, Q., Li, Y., Liu, T., Huang, D., Zheng, J., Zhu, W., Hu, M., Wu, Y., Lou, S., Hallquist, Å. M., Hallquist, M., Chan, C. K.,
471 Canonaco, F., Prévôt, A. S. H., Fung, J. C. H., Lau, A. K. H., and Yu, J. Z.: Characterization of Aerosol Aging Potentials at
472 Suburban Sites in Northern and Southern China Utilizing a Potential Aerosol Mass (Go:PAM) Reactor and an Aerosol Mass
473 Spectrometer, *Journal of Geophysical Research: Atmospheres*, 124, 5629-5649, 10.1029/2018jd029904, 2019a.
- 474 Li, J., Gao, W., Cao, L., Xiao, Y., Zhang, Y., Zhao, S., Liu, Z., Liu, Z., Tang, G., Ji, D., bo, H., Song, T., He, L., Hu, M., and Wang,



- 475 Y.: Significant changes in autumn and winter aerosol composition and sources in Beijing from 2012 to 2018: effects of clean
476 air actions, *Environmental pollution*, 115855, 10.1016/j.envpol.2020.115855, 2020a.
- 477 Li, J., Liu, Z., Gao, W., Tang, G., Hu, B., Ma, Z., and Wang, Y.: Insight into the formation and evolution of secondary organic
478 aerosol in the megacity of Beijing, China, *Atmospheric Environment*, 220, 117070, 10.1016/j.atmosenv.2019.117070, 2020b.
- 479 Li, K., Jacob, D. J., Liao, H., Shen, L., Zhang, Q., and Bates, K. H.: Anthropogenic drivers of 2013–2017 trends in summer
480 surface ozone in China, *Proceedings of the National Academy of Sciences of the United States of America*, 116, 422–427,
481 10.1073/pnas.1812168116, 2019b.
- 482 Lim, C. Y., Hagan, D. H., Coggon, M. M., Koss, A. R., Sekimoto, K., de Gouw, J., Warneke, C., Cappa, C. D., and Kroll, J. H.:
483 Secondary organic aerosol formation from the laboratory oxidation of biomass burning emissions, *Atmospheric Chemistry
484 And Physics*, 19, 12797–12809, 10.5194/acp-19-12797-2019, 2019.
- 485 Liu, T., Wang, X., Deng, W., Hu, Q., Ding, X., Zhang, Y., He, Q., Zhang, Z., Lü, S., Bi, X., Chen, J., and Yu, J.: Secondary organic
486 aerosol formation from photochemical aging of light-duty gasoline vehicle exhausts in a smog chamber, *Atmospheric
487 Chemistry and Physics*, 15, 9049–9062, 10.5194/acp-15-9049-2015, 2015.
- 488 Liu, T., Li, Z., Chan, M., and Chan, C. K.: Formation of secondary organic aerosols from gas-phase emissions of heated
489 cooking oils, *Atmospheric Chemistry and Physics*, 17, 7333–7344, 10.5194/acp-17-7333-2017, 2017a.
- 490 Liu, T., Liu, Q., Li, Z., Huo, L., Chan, M., Li, X., Zhou, Z., and Chan, C. K.: Emission of volatile organic compounds and production
491 of secondary organic aerosol from stir-frying spices, *Science of The Total Environment*, 599–600, 1614–1621,
492 10.1016/j.scitotenv.2017.05.147, 2017b.
- 493 Liu, T., Wang, Z., Huang, D. D., Wang, X., and Chan, C. K.: Significant Production of Secondary Organic Aerosol from
494 Emissions of Heated Cooking Oils, *Environmental Science & Technology Letters*, 5, 32–37, 10.1021/acs.estlett.7b00530,
495 2017c.
- 496 Liu, T., Wang, Z., Wang, X., and Chan, C. K.: Primary and secondary organic aerosol from heated cooking oil emissions,
497 *Atmospheric Chemistry and Physics*, 18, 11363–11374, 10.5194/acp-18-11363-2018, 2018.
- 498 Liu, T., Zhou, L., Liu, Q., Lee, B. P., Yao, D., Lu, H., Lyu, X., Guo, H., and Chan, C. K.: Secondary Organic Aerosol Formation
499 from Urban Roadside Air in Hong Kong, *Environmental science & technology*, 53, 3001–3009, 10.1021/acs.est.8b06587,
500 2019.
- 501 Mao, J., Ren, X., Brune, W. H., Olson, J. R., Crawford, J. H., Fried, A., Huey, L. G., Cohen, R. C., Heikes, B., Singh, H. B., Blake,
502 D. R., Sachse, G. W., Diskin, G. S., Hall, S. R., and Shetter, R. E.: Airborne measurement of OH reactivity during INTEX-B,
503 *Atmospheric Chemistry And Physics*, 9, 163–173, 10.5194/acp-9-163-2009, 2009.
- 504 Masuda, M., Wang, Q., Tokumura, M., Miyake, Y., and Amagai, T.: Risk assessment of polycyclic aromatic hydrocarbons and
505 their chlorinated derivatives produced during cooking and released in exhaust gas, *Ecotoxicology and environmental safety*,
506 197, 110592, 10.1016/j.ecoenv.2020.110592, 2020.
- 507 Matsui, H., Koike, M., Takegawa, N., Kondo, Y., Griffin, R. J., Miyazaki, Y., Yokouchi, Y., and Ohara, T.: Secondary organic
508 aerosol formation in urban air: Temporal variations and possible contributions from unidentified hydrocarbons, *Journal of
509 Geophysical Research*, 114, 10.1029/2008jd010164, 2009.
- 510 Mohr, C., DeCarlo, P. F., Heringa, M. F., Chirico, R., Slowik, J. G., Richter, R., Reche, C., Alastuey, A., Querol, X., Seco, R.,
511 Penuelas, J., Jimenez, J. L., Crippa, M., Zimmermann, R., Baltensperger, U., and Prevot, A. S. H.: Identification and
512 quantification of organic aerosol from cooking and other sources in Barcelona using aerosol mass spectrometer data,
513 *Atmospheric Chemistry And Physics*, 12, 1649–1665, 10.5194/acp-12-1649-2012, 2012.
- 514 Nah, T., Kessler, S. H., Daumit, K. E., Kroll, J. H., Leone, S. R., and Wilson, K. R.: OH-initiated oxidation of sub-micron
515 unsaturated fatty acid particles, *Physical chemistry chemical physics : PCCP*, 15, 18649–18663, 10.1039/c3cp52655k, 2013.
- 516 Nash, D. G., Baer, T., and Johnston, M. V.: Aerosol mass spectrometry: An introductory review, *International Journal of Mass
517 Spectrometry*, 258, 2–12, 10.1016/j.ijms.2006.09.017, 2006.
- 518 Ng, N. L., Canagaratna, M. R., Zhang, Q., Jimenez, J. L., Tian, J., Ulbrich, I. M., Kroll, J. H., Docherty, K. S., Chhabra, P. S.,
519 Bahreini, R., Murphy, S. M., Seinfeld, J. H., Hildebrandt, L., Donahue, N. M., DeCarlo, P. F., Lanz, V. A., Prévôt, A. S. H., Dinar,
520 E., Rudich, Y., and Worsnop, D. R.: Organic aerosol components observed in Northern Hemispheric datasets from Aerosol
521 Mass Spectrometry, *Atmospheric Chemistry and Physics*, 10, 4625–4641, 10.5194/acp-10-4625-2010, 2010.
- 522 Ng, N. L., Canagaratna, M. R., Jimenez, J. L., Zhang, Q., Ulbrich, I. M., and Worsnop, D. R.: Real-Time Methods for Estimating
523 Organic Component Mass Concentrations from Aerosol Mass Spectrometer Data, *Environmental science & technology*, 45,



- 524 910-916, 10.1021/es102951k, 2011.
- 525 Nordin, E. Z., Eriksson, A. C., Roldin, P., Nilsson, P. T., Carlsson, J. E., Kajos, M. K., Hellen, H., Wittbom, C., Rissler, J., Londahl,
526 J., Swietlicki, E., Svenningsson, B., Bohgard, M., Kulmala, M., Hallquist, M., and Pagels, J. H.: Secondary organic aerosol
527 formation from idling gasoline passenger vehicle emissions investigated in a smog chamber, *Atmospheric Chemistry And*
528 *Physics*, 13, 6101-6116, 10.5194/acp-13-6101-2013, 2013.
- 529 Peng, J., Hu, M., Du, Z., Wang, Y., Zheng, J., Zhang, W., Yang, Y., Qin, Y., Zheng, R., Xiao, Y., Wu, Y., Lu, S., Wu, Z., Guo, S.,
530 Mao, H., and Shuai, S.: Gasoline aromatics: a critical determinant of urban secondary organic aerosol formation, *Atmospheric*
531 *Chemistry and Physics*, 17, 10743-10752, 10.5194/acp-17-10743-2017, 2017.
- 532 Peng, Z., Day, D. A., Ortega, A. M., Palm, B. B., Hu, W., Stark, H., Li, R., Tsigaridis, K., Brune, W. H., and Jimenez, J. L.: Non-
533 OH chemistry in oxidation flow reactors for the study of atmospheric chemistry systematically examined by modeling,
534 *Atmospheric Chemistry and Physics*, 16, 4283-4305, 10.5194/acp-16-4283-2016, 2016.
- 535 Presto, A. A., Gordon, T. D., and Robinson, A. L.: Primary to secondary organic aerosol: evolution of organic emissions from
536 mobile combustion sources, *Atmospheric Chemistry and Physics*, 14, 5015-5036, 10.5194/acp-14-5015-2014, 2014.
- 537 Qin, Y. M., Tan, H. B., Li, Y. J., Schurman, M. I., Li, F., Canonaco, F., Prevot, A. S. H., and Chan, C. K.: Impacts of traffic emissions
538 on atmospheric particulate nitrate and organics at a downwind site on the periphery of Guangzhou, China, *Atmospheric*
539 *Chemistry And Physics*, 17, 10245-10258, 10.5194/acp-17-10245-2017, 2017.
- 540 Reyes-Villegas, E., Bannan, T., Le Breton, M., Mehra, A., Priestley, M., Percival, C., Coe, H., and Allan, J. D.: Online Chemical
541 Characterization of Food-Cooking Organic Aerosols: Implications for Source Apportionment, *Environmental science &*
542 *technology*, 52, 5308-5318, 10.1021/acs.est.7b06278, 2018.
- 543 Rogge, W. F., Hildemann, L. M., Mazurek, M. A., Cass, G. R., and Simoneit, B. R. T.: SOURCES OF FINE ORGANIC AEROSOL .1.
544 CHARBROILERS AND MEAT COOKING OPERATIONS, *Environmental science & technology*, 25, 1112-1125,
545 10.1021/es00018a015, 1991.
- 546 Rogge, W. F., Hildemann, L. M., Mazurek, M. A., Cass, G. R., and Simoneit, B. R. T.: SOURCES OF FINE ORGANIC AEROSOL .2.
547 NONCATALYST AND CATALYST-EQUIPPED AUTOMOBILES AND HEAVY-DUTY DIESEL TRUCKS, *Environmental science &*
548 *technology*, 27, 636-651, 10.1021/es00041a007, 1993.
- 549 Schauer, J. J., Kleeman, M. J., Cass, G. R., and Simoneit, B. R. T.: Measurement of emissions from air pollution sources. 4. C-
550 1-C-27 organic compounds from cooking with seed oils, *Environmental science & technology*, 36, 567-575,
551 10.1021/es002053m, 2002.
- 552 Seow, A., Poh, W. T., Teh, M., Eng, P., Wang, Y. T., Tan, W. C., Yu, M. C., and Lee, H. P.: Fumes from meat cooking and lung
553 cancer risk in Chinese women, *Cancer Epidemiol. Biomarkers Prev.*, 9, 1215-1221, 2000.
- 554 Suarez-Bertoa, R., Zardini, A. A., Platt, S. M., Hellebust, S., Pieber, S. M., El Haddad, I., Temime-Roussel, B., Baltensperger, U.,
555 Marchand, N., Prévôt, A. S. H., and Astorga, C.: Primary emissions and secondary organic aerosol formation from the exhaust
556 of a flex-fuel (ethanol) vehicle, *Atmospheric Environment*, 117, 200-211, 10.1016/j.atmosenv.2015.07.006, 2015.
- 557 Sun, Y. L., Zhang, Q., Schwab, J. J., Demerjian, K. L., Chen, W. N., Bae, M. S., Hung, H. M., Hogrefe, O., Frank, B., Rattigan, O.
558 V., and Lin, Y. C.: Characterization of the sources and processes of organic and inorganic aerosols in New York city with a
559 high-resolution time-of-flight aerosol mass spectrometer, *Atmospheric Chemistry and Physics*, 11, 1581-1602,
560 10.5194/acp-11-1581-2011, 2011.
- 561 Sun, Y. L., Zhang, Q., Schwab, J. J., Chen, W. N., Bae, M. S., Hung, H. M., Lin, Y. C., Ng, N. L., Jayne, J., Massoli, P., Williams, L.
562 R., and Demerjian, K. L.: Characterization of near-highway submicron aerosols in New York City with a high-resolution
563 aerosol mass spectrometer, *Atmospheric Chemistry And Physics*, 12, 2215-2227, 10.5194/acp-12-2215-2012, 2012.
- 564 Tang, R. Z., Wang, H., Liu, Y., and Guo, S.: Constituents of Atmospheric Semi-Volatile and Intermediate Volatility Organic
565 Compounds and Their Contribution to Organic Aerosol, *Prog. Chem.*, 31, 180-190, 10.7536/pc180431, 2019.
- 566 Timonen, H., Karjalainen, P., Saukko, E., Saarikoski, S., Aakko-Saksa, P., Simonen, P., Murtonen, T., Dal Maso, M., Kuuluvainen,
567 H., Bloss, M., Ahlberg, E., Svenningsson, B., Pagels, J., Brune, W. H., Keskinen, J., Worsnop, D. R., Hillamo, R., and Rönkkö, T.:
568 Influence of fuel ethanol content on primary emissions and secondary aerosol formation potential for a modern flex-fuel
569 gasoline vehicle, *Atmospheric Chemistry and Physics*, 17, 5311-5329, 10.5194/acp-17-5311-2017, 2017.
- 570 Tkacik, D. S., Lambe, A. T., Jathar, S., Li, X., Presto, A. A., Zhao, Y., Blake, D., Meinardi, S., Jayne, J. T., Croteau, P. L., and
571 Robinson, A. L.: Secondary organic aerosol formation from in-use motor vehicle emissions using a potential aerosol mass
572 reactor, *Environmental science & technology*, 48, 11235-11242, 10.1021/es502239v, 2014.



- 573 Ulbrich, I. M., Canagaratna, M. R., Zhang, Q., Worsnop, D. R., and Jimenez, J. L.: Interpretation of organic components from
574 Positive Matrix Factorization of aerosol mass spectrometric data, *Atmospheric Chemistry And Physics*, 9, 2891-2918,
575 10.5194/acp-9-2891-2009, 2009.
- 576 Volkamer, R., Jimenez, J. L., San Martini, F., Dzepina, K., Zhang, Q., Salcedo, D., Molina, L. T., Worsnop, D. R., and Molina, M.
577 J.: Secondary organic aerosol formation from anthropogenic air pollution: Rapid and higher than expected, *Geophysical*
578 *Research Letters*, 33, 10.1029/2006gl026899, 2006.
- 579 Wang, T., Xue, L., Brimblecombe, P., Lam, Y. F., Li, L., and Zhang, L.: Ozone pollution in China: A review of concentrations,
580 meteorological influences, chemical precursors, and effects, *The Science of the total environment*, 575, 1582-1596,
581 10.1016/j.scitotenv.2016.10.081, 2017.
- 582 Watne, A. K., Psichoudaki, M., Ljungstrom, E., Le Breton, M., Hallquist, M., Jerksjo, M., Fallgren, H., Jutterstrom, S., and
583 Hallquist, A. M.: Fresh and Oxidized Emissions from In-Use Transit Buses Running on Diesel, Biodiesel, and CNG,
584 *Environmental science & technology*, 52, 7720-7728, 10.1021/acs.est.8b01394, 2018.
- 585 Wu, Y., Zhang, S., Hao, J., Liu, H., Wu, X., Hu, J., Walsh, M. P., Wallington, T. J., Zhang, K. M., and Stevanovic, S.: On-road
586 vehicle emissions and their control in China: A review and outlook, *The Science of the total environment*, 574, 332-349,
587 10.1016/j.scitotenv.2016.09.040, 2017.
- 588 Yu, Y., Wang, H., Wang, T., Song, K., Tan, T., Wan, Z., Gao, Y., Dong, H., Chen, S., Zeng, L., Hu, M., Wang, H., Lou, S., Zhu, W.,
589 and Guo, S.: Elucidating the importance of semi-volatile organic compounds to secondary organic aerosol formation at a
590 regional site during the EXPLORE-YRD campaign, *Atmospheric Environment*, 118043, 10.1016/j.atmosenv.2020.118043,
591 2020.
- 592 Zeng, J., Yu, Z., Mekić, M., Liu, J., Li, S., Loisel, G., Gao, W., Gandolfo, A., Zhou, Z., Wang, X., Herrmann, H., Gligorovski, S.,
593 and Li, X.: Evolution of Indoor Cooking Emissions Captured by Using Secondary Electrospray Ionization High-Resolution
594 Mass Spectrometry, *Environmental Science & Technology Letters*, 7, 76-81, 10.1021/acs.estlett.0c00044, 2020.
- 595 Zhang, Q., Worsnop, D. R., Canagaratna, M. R., and Jimenez, J. L.: Hydrocarbon-like and oxygenated organic aerosols in
596 Pittsburgh: insights into sources and processes of organic aerosols, *Atmospheric Chemistry And Physics*, 5, 3289-3311,
597 10.5194/acp-5-3289-2005, 2005.
- 598 Zhang, Q., Jimenez, J. L., Canagaratna, M. R., Ulbrich, I. M., Ng, N. L., Worsnop, D. R., and Sun, Y.: Understanding atmospheric
599 organic aerosols via factor analysis of aerosol mass spectrometry: a review, *Analytical and Bioanalytical Chemistry*, 401,
600 3045-3067, 10.1007/s00216-011-5355-y, 2011.
- 601 Zhang, R., Wang, G., Guo, S., Zamora, M. L., Ying, Q., Lin, Y., Wang, W., Hu, M., and Wang, Y.: Formation of urban fine
602 particulate matter, *Chemical reviews*, 115, 3803-3855, 10.1021/acs.chemrev.5b00067, 2015.
- 603 Zhang, Y., Deng, W., Hu, Q., Wu, Z., Yang, W., Zhang, H., Wang, Z., Fang, Z., Zhu, M., Li, S., Song, W., Ding, X., and Wang, X.:
604 Comparison between idling and cruising gasoline vehicles in primary emissions and secondary organic aerosol formation
605 during photochemical ageing, *The Science of the total environment*, 722, 137934, 10.1016/j.scitotenv.2020.137934, 2020a.
- 606 Zhang, Z., Zhu, W., Hu, M., Wang, H., Chen, Z., Shen, R., Yu, Y., Tan, R., and Guo, S.: Secondary Organic Aerosol from Typical
607 Chinese Domestic Cooking Emissions, *Environmental Science & Technology Letters*, 10.1021/acs.estlett.0c00754, 2020b.
- 608 Zhao, Y., Nguyen, N. T., Presto, A. A., Hennigan, C. J., May, A. A., and Robinson, A. L.: Intermediate Volatility Organic
609 Compound Emissions from On-Road Diesel Vehicles: Chemical Composition, Emission Factors, and Estimated Secondary
610 Organic Aerosol Production, *Environmental science & technology*, 49, 11516-11526, 10.1021/acs.est.5b02841, 2015.
- 611 Zhao, Y., Lambe, A. T., Saleh, R., Saliba, G., and Robinson, A. L.: Secondary Organic Aerosol Production from Gasoline Vehicle
612 Exhaust: Effects of Engine Technology, Cold Start, and Emission Certification Standard, *Environmental science & technology*,
613 52, 1253-1261, 10.1021/acs.est.7b05045, 2018.
- 614 Zhao, Y. L., Hu, M., Slanina, S., and Zhang, Y. H.: Chemical compositions of fine particulate organic matter emitted from
615 Chinese cooking, *Environmental science & technology*, 41, 99-105, 10.1021/es0614518, 2007.
- 616 Zhao, Y. L., Saleh, R., Saliba, G., Presto, A. A., Gordon, T. D., Drozd, G. T., Goldstein, A. H., Donahue, N. M., and Robinson, A.
617 L.: Reducing secondary organic aerosol formation from gasoline vehicle exhaust, *Proceedings of the National Academy of*
618 *Sciences of the United States of America*, 114, 6984-6989, 10.1073/pnas.1620911114, 2017.
- 619 Zhong, L. J., Goldberg, M. S., Gao, Y. T., and Jin, F.: Lung cancer and indoor air pollution arising from Chinese style cooking
620 among nonsmoking women living in Shanghai, China, *Epidemiology*, 10, 488-494, 10.1097/00001648-199909000-00005,
621 1999.



622 Zhou, W., Xu, W., Kim, H., Zhang, Q., Fu, P., Worsnop, D. R., and Sun, Y.: A review of aerosol chemistry in Asia: insights from
623 aerosol mass spectrometer measurements, *Environmental science. Processes & impacts*, 10.1039/d0em00212g, 2020.

624

625

626

627

628

629

630

631

632

633

634

635

636

637

638

639

640

641

642

643

644

645

646

647

648

649

650

651

652

653

654



Table 1. Descriptions of vehicle exhaust and sampling procedures.

Experiment	Revolving Speed	Torque	Sampling Time	Parallels	Particle Density	Fuel	Sampling Line Temperature
GDI 20 km/h	1500 Hz	16 N·m	60 min	3~5			
GDI 40 km/h	2000 Hz	16 N·m	70 min	3~6	1.1~1.2 g/cm ³	Gasoline (China V, similar to Euro V)	20~25°C
GDI 60 km/h	1750 Hz	32 N·m	60 min	3~5			

655

656

657

658

659

660

661

662

663

664

665

666

667

668

669

670



Table 2. Descriptions of cooking emission and sampling procedures.

Experiment	Cooking Material	Oil Temperature	Total Cooking Time	Number of Dishes	Sampling Time	Parallels	Particle Density	Fuel & Cooware	Kitchen Volume	Sampling Line Temperature
Deep-fried Meat	170 g chicken, 500 ml corn oil and a few condiments	145~155°C	66 min	5	90 min	3~8	1.11±0.02 g/cm ³			
Shallow-fried Tofu	500 g tofu, 200 ml corn oil and a few condiments	100~110°C	64 min	5	60 min	3~5	1.04±0.03 g/cm ³	Liquefied petroleum gas (LPG) & iron wok	78 m ³ (5.6 m × 4 m × 3.5 m)	20~25°C
Stir-fried Cabbage	300 g cabbage, 40 ml corn oil and a few condiments	95~105°C	47 min	5	58 min	3~5	1.16±0.03 g/cm ³			
Kung Pao Chicken	150 g chicken, 50 g ceanut, 50 g cucumber, 40 ml corn oil and a few condiments	Unmeasured ^a	40 min	5	60 min	3~5	1.07±0.02 g/cm ³			

^aIt is need to stir constantly, so the oil temperature was unstable.

671

672

673

674

675

676

677

678

679

680



Table 3. The Go: PAM condition for vehicle experiment.

Experiment	O ₃ concentration (ppbV)	OH Exposure ^a ($\times 10^{10}$ molecules·cm ⁻³ ·s)	Photochemical Age (days, [OH]= 1.5×10^6 molecules·cm ⁻³)	External OH reactivity of SO ₂ during offline calibration (S ⁻¹)	External OH reactivity of VOCs during experiment (S ⁻¹)	Ratio of OH Exposure calculated by an estimator ^b to that calculated by the decay of SO ₂ ^a	Temperature & RH in Go: PAM	Basic Description of Go: PAM	Wall Loss
	624	7.79	0.6						
	2367	21.4	1.7						
GDI 20 km/h	4433	37.4	2.9		10.4	119%			
	6533	53.8	4.2						
	8050	65.6	5.1	15.8			Temp: 19~22°C RH: 44-49%	Voluem: 7.9 L, Flow rate: 4 L/min for sample air and 1 L/min for sheath gas. Residence time: 110 s.	The wall loss of particle have been adjusted in each size bin measured by two synchronous SMPS (two SMPS runned before and after Go: PAM respectively).The wall loss of gas phase is minor according to previous reseach.
GDI 40 km/h	8701	70.6	5.5						
	The same as 20 km/h experiments								
GDI 60 km/h	The same as 20 km/h experiments								
	The same as 20 km/h experiments								

^aOH exposure was calculated based on the decay of SO₂.

^bOH exposure for each ingredient was calculated based on the OFR estimator.



Table 4. The Go: PAM condition for cooking experiment.

Experiment	O ₃ concentration (ppbV)	OH Exposure ^a ($\times 10^{10}$ molecules \cdot cm ⁻³ \cdot s)	Photochemical Age (days, [OH]= 1.5×10^6 molecules \cdot cm ⁻³)	External OH reactivity of SO ₂ during offline calibration (S ⁻¹)	External OH reactivity of VOCs during experiment (S ⁻¹)	Ratio of OH Exposure calculated by an estimator ^b to that calculated by the decay of SO ₂ ^a	Temperature & RH in Go: PAM	Basic Description of Go: PAM	Wall Loss
	-	0	0.0						
Deep-fried Chicken	310	4.3	0.3		25.7	97%			The wall loss of particle have been adjusted in each size bin measured by two synchronous
Shallow-fried Tofu	1183	9.6	0.7				Temp: 16~19°C RH: 18~23%	Voluem: 7.9 L. Flow rate: 7 L/min for sample air and SMPS (two SMPS runned before and after Go: PAM sheath gas. Residence time: respectively). The wall loss of gas phase is minor according to previous reseach.	
Stir-fried Cabbage	2217	14.4	1.1	24.0	21.7	111%			
Kung Pao Chicken	3267	21.4	1.7		23.3	104%			
	4025	27.1	2.1		23.6	103%			
	The same as Meat experiments								
	The same as Meat experiments								
	The same as Meat experiments								

^aOH exposure was calculated based on the decay of SO₂.
^bOH exposure for each ingredient was calculated based on the OFR estimator.



Table 5. A summary of elemental ratios and dominant peaks among various SOA.

Type	O/C	H/C	f_{28}	f_{29}	f_{41}	f_{43}	f_{44}	f_{55}	f_{57}	Dominant Peaks (In decreasing order)
GDI LO-OOA	0.46	1.80	0.066	0.076	0.051	0.133	0.077	0.043	0.029	m/z 43, 44, 29, 28, 41, 55
GDI MO-OOA	0.91	1.57	0.134	0.071	0.026	0.117	0.146	0.024	0.013	m/z 44, 28, 43, 29, 45, 27
Cooking LO-OOA	0.36	1.92	0.053	0.065	0.058	0.097	0.065	0.056	0.046	m/z 43, 44, 29, 41, 55, 28
Heated oil SOA (Liu, 2018)	0.38	1.53	0.070	0.087	0.067	0.078	0.067	0.053	0.023	m/z 29, 43, 28, 44, 41, 55
Meat charbroiling SOA (Kaltsonoudis, 2017)	0.24	1.83	0.039	0.061	0.077	0.075	0.052	0.074	0.035	m/z 41, 43, 55, 29, 27, 44
Gasoline SOA (Nordin, 2013)	0.40	1.38	0.122	0.032	0.031	0.094	0.129	0.019	0.008	m/z 44, 28, 39, 27, 29, 41
Diesel SOA (Chirico, 2010)	0.37	1.57	0.069	0.092	0.062	0.112	0.073	0.045	0.022	m/z 43, 29, 44, 28, 41, 27

Table 6. Pearson correlations between lab OA and ambient OA mass spectra.

Pearson Correlation ($\alpha=0.05$)	Ambient HOA	Ambient COA	Ambient LO-OOA	Ambient MO-OOA
Lab Cooking POA	0.95	0.86	0.46	0.39
Lab Cooking LO-OOA	0.90	0.81	0.76	0.68
Lab Vehicle LO-OOA	0.80	0.71	0.81	0.73
Lab Vehicle MO-OOA	0.54	0.44	0.98	0.94

701

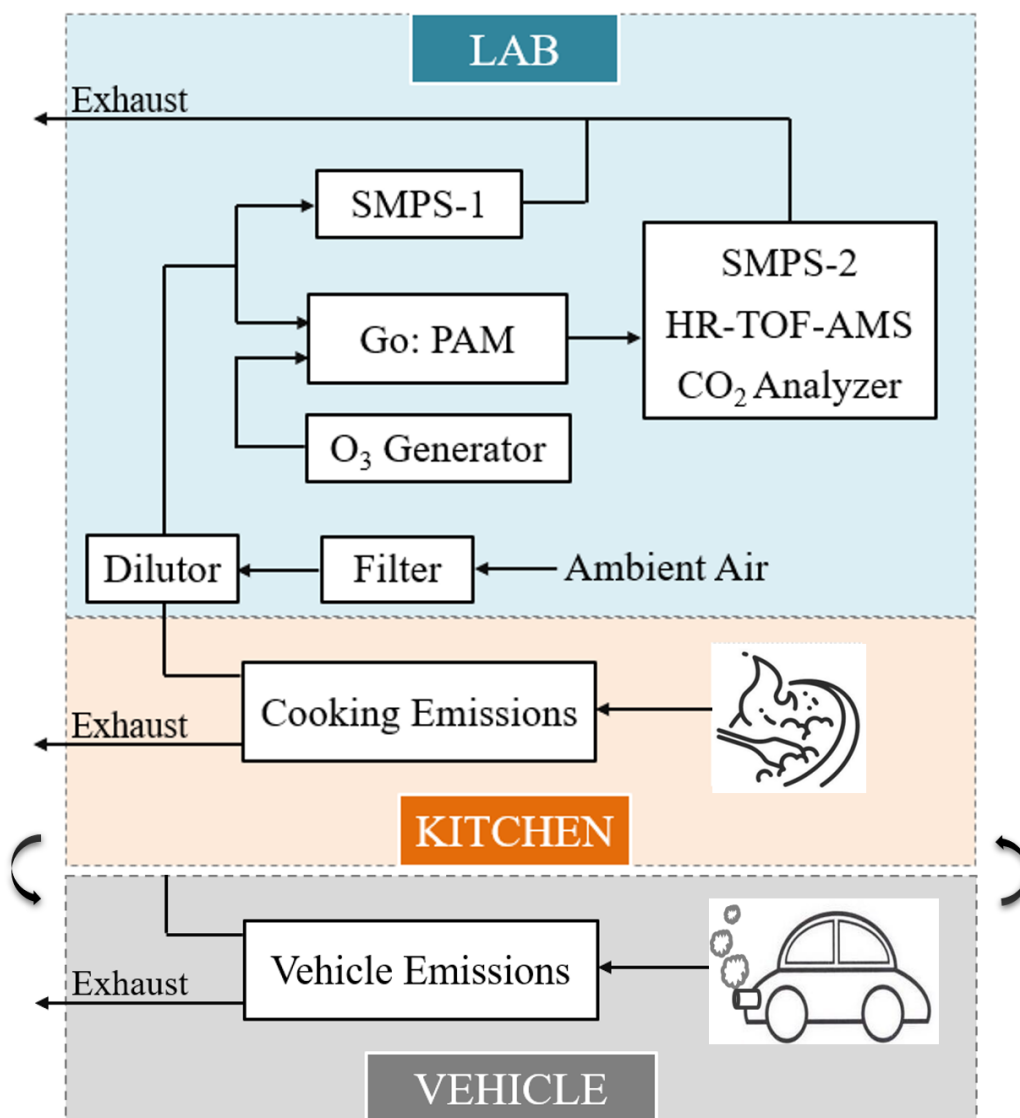
702

703

704

705

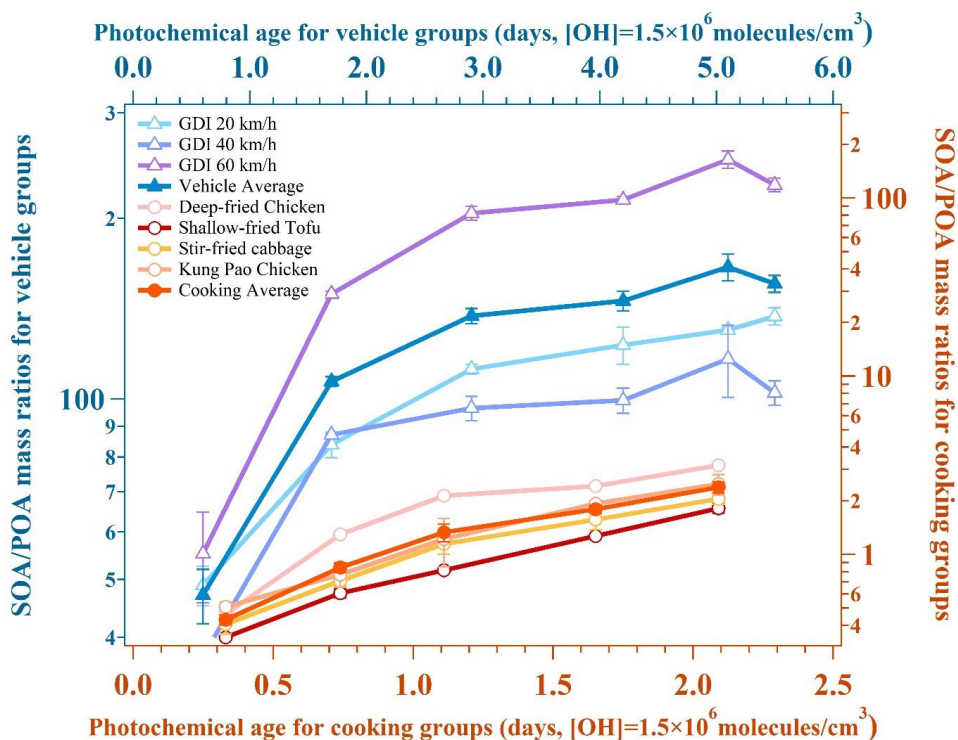
706



707

708 **Figure 1.** Schematic of experiment system.

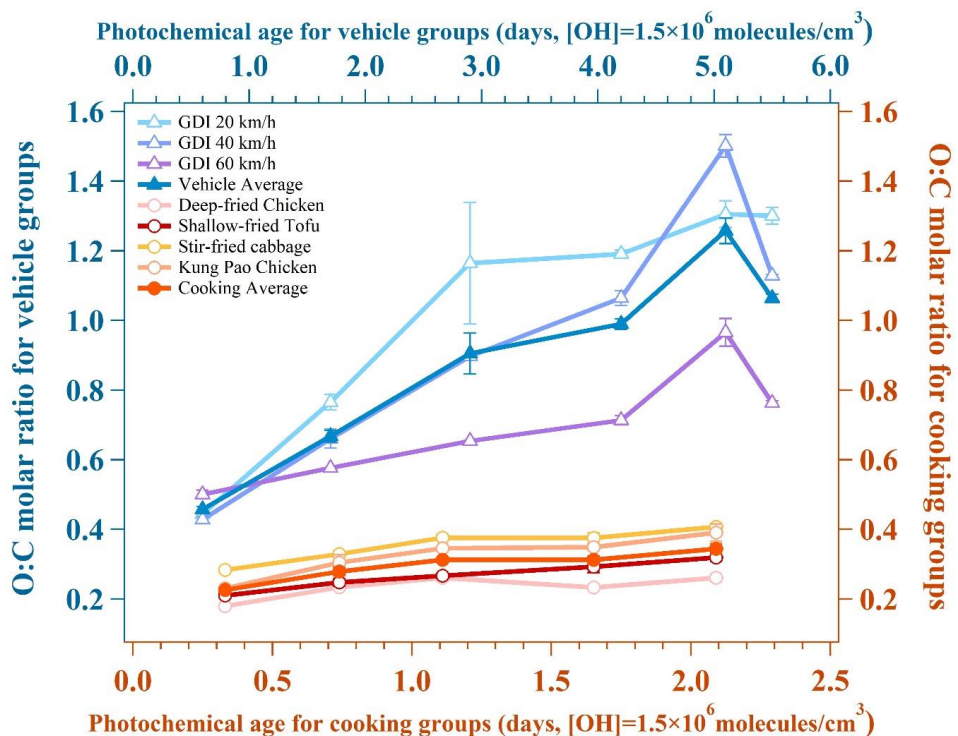
709



710

711

Figure 2. Mass growth potentials for two urban lifestyle SOA.

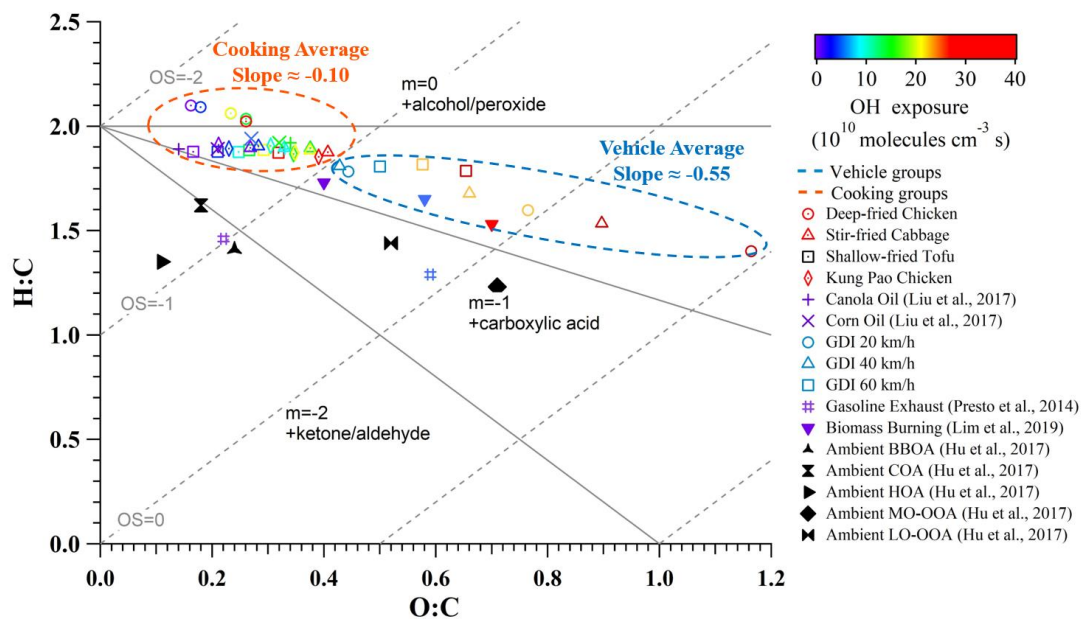


712

713

714

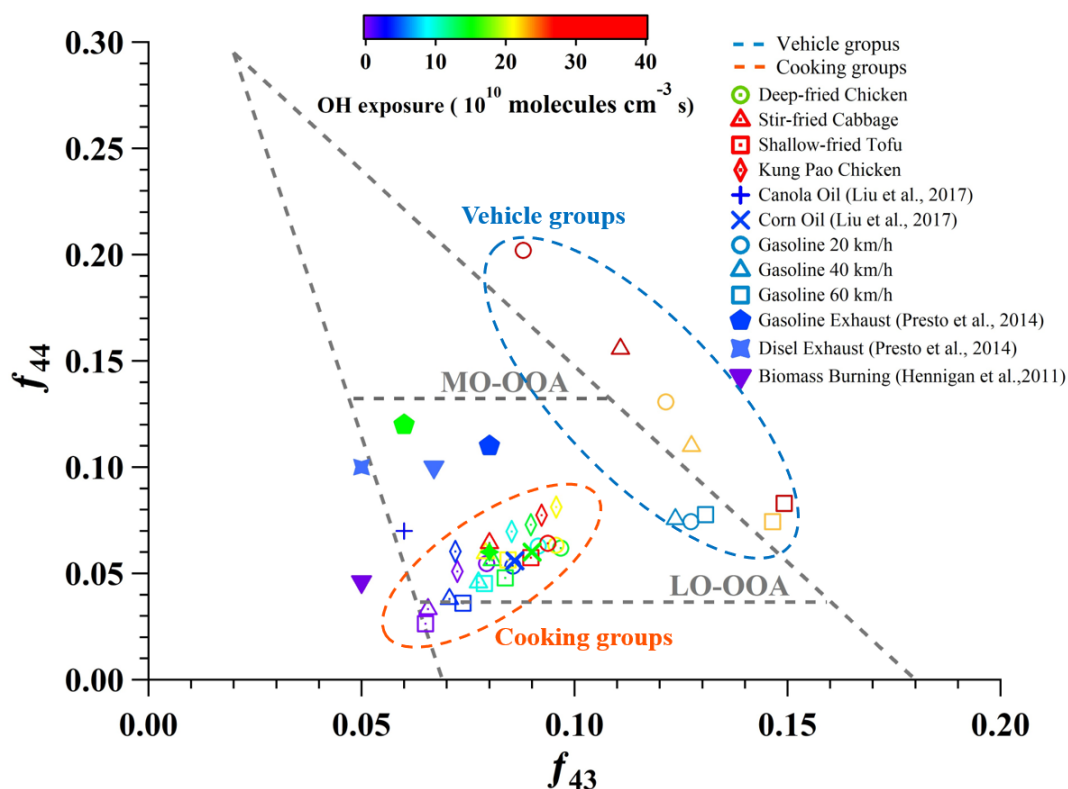
Figure 3. Evolution of O:C molar ratio for two urban lifestyle SOA.



715

716 **Figure 4.** Van Krevelen diagram of OA from various sources.

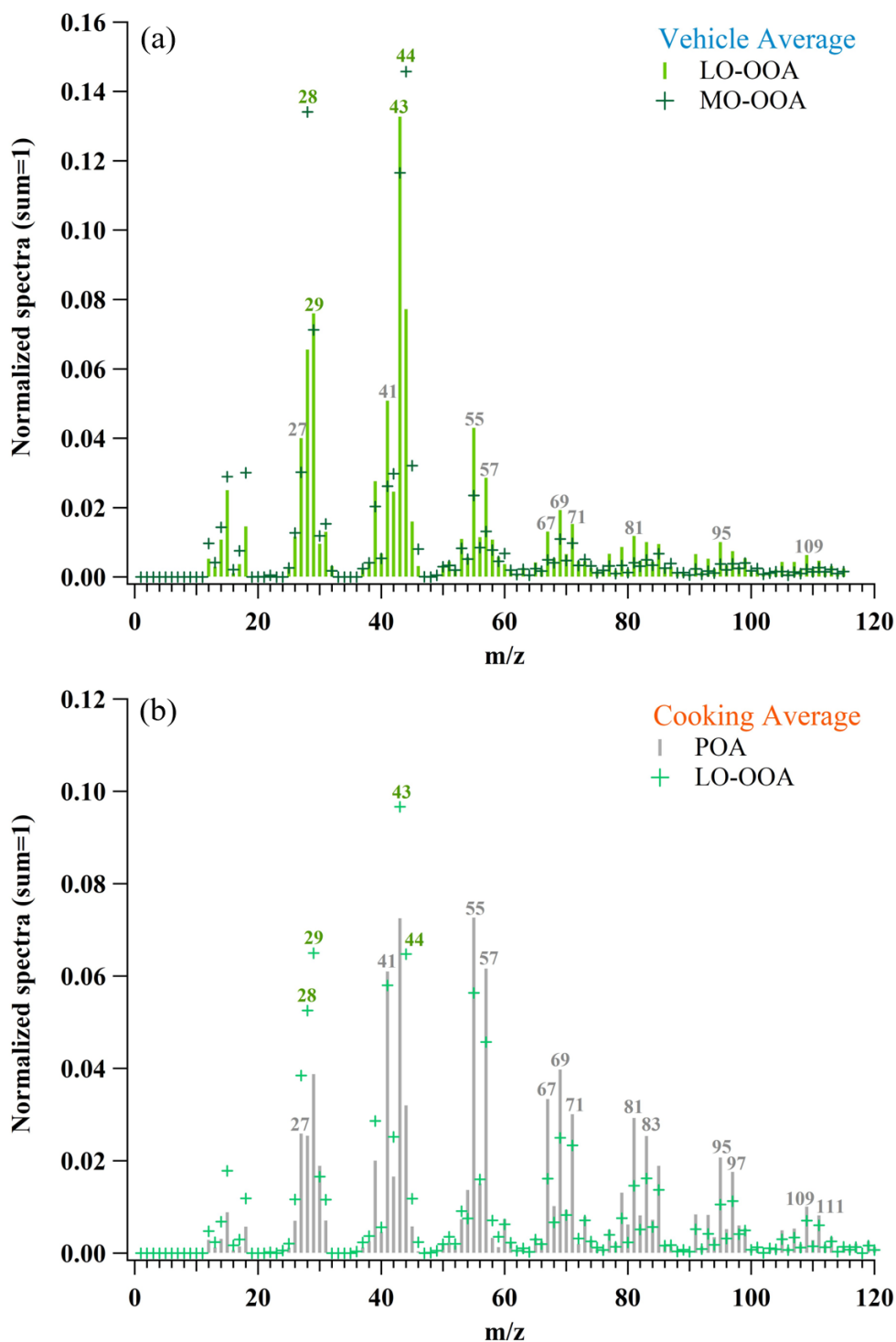
717



718

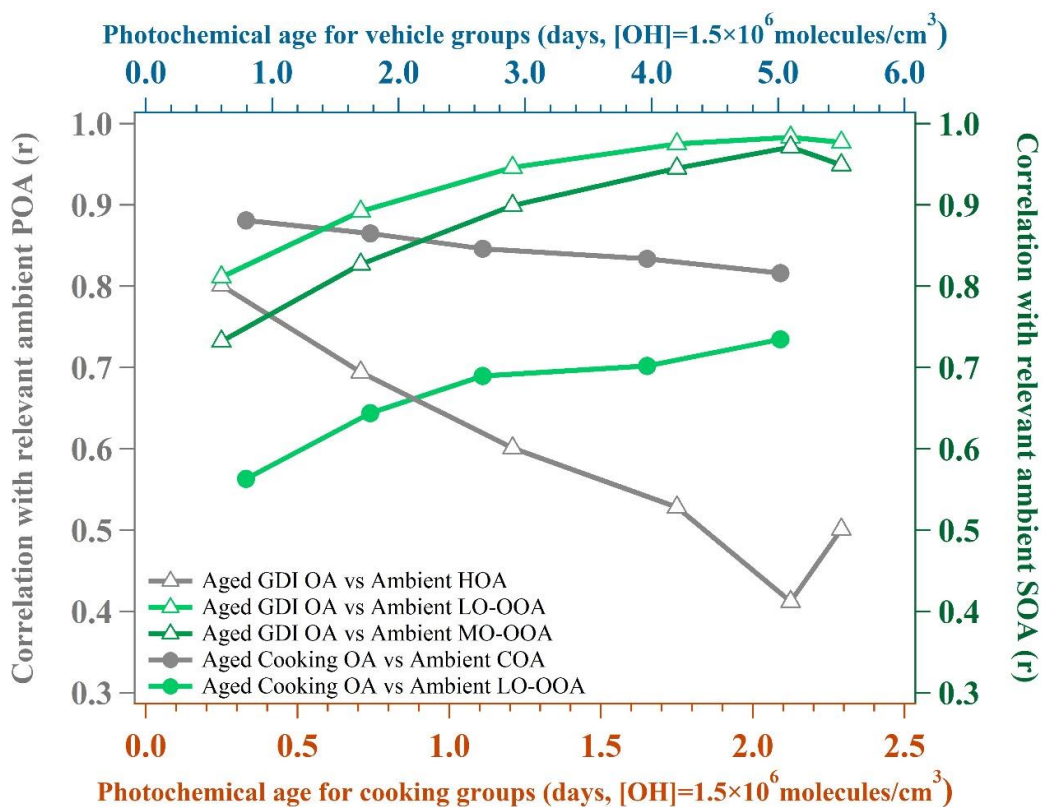
719 **Figure 5.** Fractions of entire organic signals at m/z 43 (f_{43}) vs. m/z 44 (f_{44}) from various sources as well as Ng triangle plot.

720



721

722 **Figure 6.** Average mass spectra of OA from two urban lifestyle sources.



723

724

Figure 7. Correlation coefficients (pearson r) between the lab aged OA and published ambient PMF-OA factors with growing photochemical ages. Ambient PMF-OA factors are the average results from two field studies in Beijing (Measured at a typical urban site during autumn and winter; Autumn: Oct. 1st, 2018 – Nov. 15th, 2018; Winter: Jan. 5th, 2019 – Jan. 31st, 2019).

725

726

727

728